https://doi.org/10.5194/egusphere-2026-4505
Preprint. Discussion started: 30 July 2026

Insights into Deep Mesoscale Eddy Variability in the Gulf of Mexico

Justin P. Cooke[1], Kathleen A. Donohue[1], and D. Randolph Watts[1]

[1]Graduate School of Oceanography, University of Rhode Island, Narragansett, Rhode Island

Correspondence: Justin P. Cooke (justin.cooke@uri.edu)

Abstract. Deep (>1000 m depth) barotropic mesoscale eddies contribute to Loop Current Eddy (LCE) separation events, but sparse deep observations in the Gulf of Mexico limit our dynamical understanding and forecast skill. Data from a regional HYbrid Coordinate Ocean Model (HYCOM) free-running simulation are used to analyze deep, mesoscale variability over an 18-year period in the Eastern Gulf. A spectral analysis reveals three notable frequency bands: $1/150$ - $1/60$ days^{-1}, $1/60$ - $1/30$ days^{-1}, and $1/30$ - $1/10$ days^{-1}. $60-150$ day variance is concentrated in the central Eastern Gulf and the Deep Southeast Channel (DSC), whereas $30-60$ day variance is strongest near the Mississippi Fan. Complex empirical orthogonal function analysis identifies three modes that contain 65% of the total deep variance. The first mode is associated with $30-60$ day eddies formed by baroclinic development near the Mississippi Fan and propagate into the Eastern Gulf basin, then westward; the second and third modes capture variance representative of eddies in the $60-150$ day and $10-30$ day bands. Periods of largest modal amplitudes coincide with times when the LC extends into the Gulf, indicating that the deep Eastern Gulf is energized by the LC via baroclinic development and topographic interactions. The presence of a strong deep cyclone in the DSC is associated with Modes 2 and 3; LCE separations coinciding with this feature occur south of 25°N. Insights from this work suggest greater emphasis in observing the DSC to improve the predictability of LCE separations, and our understanding of the physical mechanisms controlling these events.

1 Introduction

The Gulf of Mexico is a marginal sea bordering the United States, Mexico, and Cuba, with critical economic, ecological, and environmental importance (National Academies of Sciences and Medicine, 2018; McKinney et al., 2021). In the Gulf, the Loop Current (LC) transports warm, salty waters from the Caribbean Sea through the Yucatán Channel and exits through the Straits of Florida. This flow may remain in a retracted port-to-port configuration, or extend into the Gulf as far as 28°N and 93°W as a northward loop. A Loop Current Eddy (LCE), a closed, warm-core anticyclone with horizontal scales of 200–400 km, can pinch off from the LC. The LC and LCE may undergo multiple instances of detachment and reattachment before ultimately separating (Leben, 2005; Tsei et al., 2025), exporting strong currents and substantial energy into the Western Gulf. This cycle of extension, detachment, and separation occurs irregularly, with periods ranging from about 2 to 18 months (Sturges and Leben, 2000; Leben, 2005).

The LC system is the primary driver of mesoscale variability, both in surface and deep waters (Oey, 2008). At the surface, the eddy-rich field of LC meanders and LCEs is clearly visible in satellite sea-surface height, temperature and ocean color.

https://doi.org/10.5194/egusphere-2026-4505
Preprint. Discussion started: 30 July 2026

Below the surface, the LC's interaction with topography and associated baroclinic development generate strong deep variability, including deep mesoscale eddies (Oey, 2008; Hamilton, 2009; Donohue et al., 2016; Hamilton et al., 2016; Pérez-Brunius et al., 2018; Le Hénaff et al., 2012; Safaie et al., 2025). In the deep Eastern Gulf, observations indicate two regions of particularly elevated deep eddy energy: beneath the LC itself, where baroclinic instability is active, and near the Mississippi Fan, where the LC interacts strongly with topography and generates deep, topographic-Rossby-wave–like variability (Hamilton, 2009; Donohue et al., 2016; Hamilton et al., 2016; Pérez-Brunius et al., 2018; Johnson Exley et al., 2022).

In terms of vertical structure, Hamilton et al. (2016) showed that two vertical modes constitute $\geq 90\%$ of the variance: a surface-intensified mode and a nearly depth-independent mode. Most of the vertical structure associated with the surface-intensified mode appears in the upper ≈ 1000 m, while below this depth hydrographic properties exhibit weak lateral gradients. Thus, we adopt a simple terminology: "upper" refers to the surface-intensified mode and the steric component of sea-surface height (SSH); "deep" describes the nearly depth-independent mode.

Both models and observations broadly agree on the existence and importance of deep mesoscale eddies. Numerical simulations show deep eddies forming via LC–topography interaction and baroclinic processes (Oey, 2008; Le Hénaff et al., 2012; Safaie et al., 2025). Morey et al. (2020) compared three free-running numerical models against four years of RAFOS float data and found that the models reproduce the major features of deep currents and deep-energy "hot spots", but generally underestimate the magnitude of deep eddy energy. More recent numerical studies suggest that deep eddies can influence the timing and location of LCE separations through upper–deep interactions (Safaie et al., 2025; Thoppil et al., 2025). Emerging modeling work also points to the Deep Southeast Channel (DSC) as a dynamically important, yet observationally challenging, region where deep eddies may strongly influence LC separations (Safaie et al., 2025), and the details of this dynamical influence deserve further examination. Additionally, satellite altimeter observations reinforce the importance of this region in LC separations from a surface perspective (Larrañaga et al., 2026)

Despite these advances, direct observations of deep variability remain infrequent in space and time. RAFOS float trajectories span much of the Gulf but are too sparse to resolve the full mesoscale structure. Mesoscale mapping arrays provide dense measurements but only over limited regions and time periods. For example, the Current and Pressure Inverted Echo Sounder (CPIES) array used by Johnson Exley et al. (2022) to document LC-driven deep energy near the Mississippi Fan, though large compared to earlier efforts (Hamilton et al., 2016), was confined to 25°–27.5°N and 86°–89°W. Thus, while there is growing evidence that deep eddy variability, especially beneath the LC, near the Mississippi Fan, and in the DSC, play an important role in LC and LCE dynamics, our knowledge is built on limited, regionally focused, and relatively short observational records. There remains a significant gap in our understanding of how deep mesoscale eddies in the Gulf vary over extended time periods, and how they systematically affect the LCE separation process. Moreover, their representation impacts ensemble forecast performance (Thoppil et al., 2025; Cooke et al., 2025).

Here we investigate deep eddy variability using a 54-year free-running HYbrid Coordinate Ocean Model (HYCOM) simulation (Dukhovskoy et al., 2015). This multidecadal free-running model demonstrated realistic statistics of the LC and reasonably represented mesoscale processes (Dukhovskoy et al., 2015); further, the model deep mean circulation compared favorably to observations, and demonstrated more realistic deep eddy kinetic energy (EKE) in the Gulf against other numerical mod-

https://doi.org/10.5194/egusphere-2026-4505
Preprint. Discussion started: 30 July 2026

els (Morey et al., 2020). To extract coherent patterns from this high-dimensional system, we follow prior work and apply Complex empirical orthogonal function (CEOF) analysis.

Modal methods are well suited to isolating dynamically relevant structure from flows with expansive ranges of spatial and temporal scales (Taira et al., 2017), and have been widely used in the LC region. Empirical orthogonal function (EOF) analyses have been applied to Yucatán Channel observations to relate along- and cross-channel velocity variability to LC behavior (Abascal et al., 2003; Bunge et al., 2002; Sheinbaum et al., 2016; Manta et al., 2023), and to model fields such as relative-vorticity stretching to link deep circulation to LC variability (Oey, 2008). CEOFs extend EOFs by resolving phase, allowing identification of propagating versus standing modes. CEOF analysis has been used to study deep eddy propagation in the northern Eastern Gulf (Oey, 2008), as well as the propagation characteristics of deep signals in bottom-pressure and near-bottom current data, including topographic Rossby waves near the Mississippi Fan (Rosburg et al., 2016; Johnson Exley et al., 2022). More recently, Olvera-Prado et al. (2023) used CEOFs to study the upper-deep coupling and its variability in relation to LCE separations with data from a 21-year HYCOM free-running model; their study used layer thickness to show that dominant upper–lower layer circulation patterns in the Gulf recur on timescales of 7–14 months, tied to the LC/LCE separation cycle, with deep features like anticyclone–cyclone modons directly linked to LC extension and LCE separation. This study complements Olvera-Prado et al. (2023) by decomposing deep mesoscale variability into frequency bands and spatial modes, revealing how the LC energizes the deep eddy field.

Our approach is to analyze 18 years of HYCOM deep eddy variability using the 2000 m streamfunction, represented by the reference sea-surface height η_{ref}, and LC statistics. Spectral analysis identifies key frequency bands associated with mesoscale eddy energy: $10-30$ days (high frequency), $30-60$ days (mid frequency), and $60-150$ days (low frequency). A CEOF analysis of the deep eddy field in the Eastern Gulf reveals three leading modes that explain 65% of the variance; these modes strengthen during LC detachment and separation periods and are suppressed when the LC is retracted, implicating them in the LCE separation process. LCE separations in the presence of a strong deep cyclone are found to occur south of 25° N. These findings also contribute to improving understanding of persistent pathways of deep eddies. $10-30$ day eddies tend to propagate west along the slope of the Mississippi Fan, whereas $60-150$ day eddies propagate south towards the DSC; those in the $30-60$ day band propagate south off of the Mississippi Fan into the deep eastern basin and move west, along the bathymetry.

2 Methodology

2.1 Numerical Setup

The free-running 54-year, regional HYbrid Coordinate Ocean Model (HYCOM) simulation (Dukhovskoy et al., 2015) deploys a $1/25°$ horizontal grid and 20 hybrid layers in the vertical, and is bounded from 18.9°N to 31.96°N and 98°W to 76.4°W (see Fig. 1). A nested modeling approach is used for the lateral boundary conditions, where an open boundary condition is produced from bi-weekly climatology taken from four years of a free-running $1/12°$ Atlantic HYCOM run. The model is spun-up from a 5-year simulation using Generalized Digital Environmental Model 3.0 climatological fields forced with atmospheric fields from the Fleet Numerical Meteorology and Oceanography Center's Navy Operational Global Atmospheric Prediction System.

https://doi.org/10.5194/egusphere-2026-4505
Preprint. Discussion started: 30 July 2026

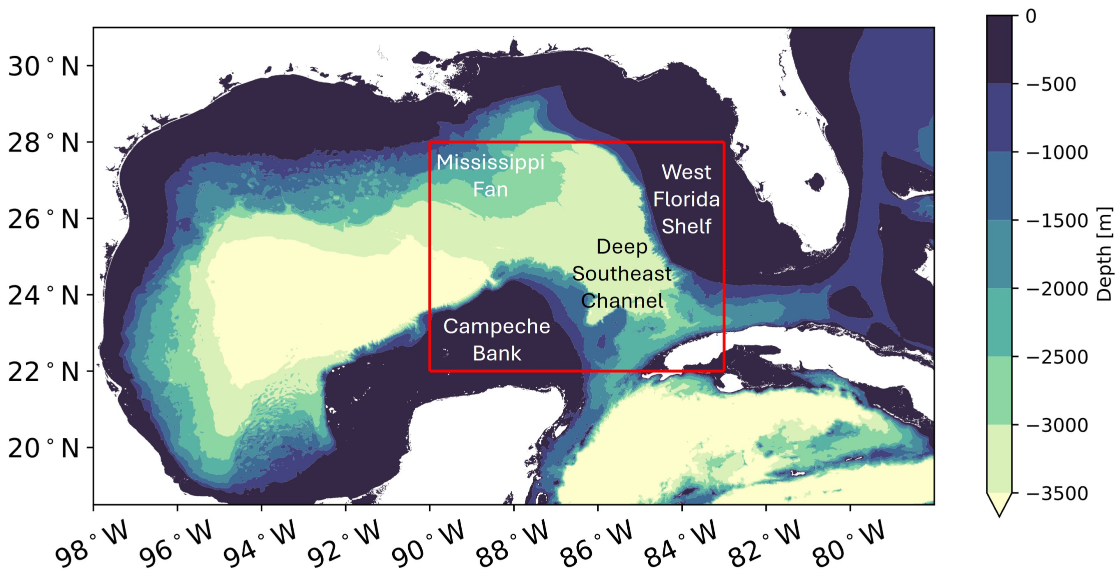

Figure 1. The Gulf of Mexico with the study's region of interest, the basin of the Eastern Gulf, bounded from 22°N to 28°N, 90°W to 83°W (red box). Bathymetry is contoured every 500 meters. Bathymetric features of interest are labeled.

After this spin-up period, atmospheric forcing is derived using 18 years (1992-2009) of hourly fields from the Climate Forecast System Reanalysis. This forcing is cycled three times, resulting in the 54-year model run. Further details of the model are included in Dukhovskoy et al. (2015) (see their Tab. 1). For our analysis we use 18-years – the first model cycle – to analyze the deep variability. Morey et al. (2020) found good agreement between deep mean currents from this HYCOM simulation and RAFOS float observations. We use available SSH and z-gridded temperature (T) and salinity (S) data from the surface to 2000 meters depth to calculate η_{steric} and η_{ref}, as outlined in the next subsection.

2.2 Identification of Deep Mesoscale Eddies

To represent deep circulation and mesoscale eddies in the model data, we calculate the deep reference pressure (η_{ref} [m]) component as the difference between the total sea surface height (η_{total} [m]) and the steric (η_{steric} [m]) components:

$$\eta_{total} = \eta_{ref} + \eta_{steric}. \tag{1}$$

Use of η_{ref} is advantageous in its simplicity – eddies are identified using this scalar stream function, as opposed to a more highly differentiated scalar parameter like relative vorticity. This stream function enables a straightforward visualization of the deep fields, allowing for the determination of deep, mesoscale features.

η_{steric} is geopotential height anomaly (ϕ) divided by g, the acceleration due to gravity. ϕ is found by integrating from the surface ($P_1 = 0$ dbar) to a constant reference pressure, $P_{ref} \approx 2023$ dbar (equivalently 2000 m depth),

https://doi.org/10.5194/egusphere-2026-4505
Preprint. Discussion started: 30 July 2026

$$\phi = \int_{P1}^{P_{ref}} \delta dP, \tag{2}$$

where δ is the specific volume anomaly,

$$\delta = \frac{1}{\rho(S,T,P)} - \frac{1}{\rho(S_0,T_0,P)}. \tag{3}$$

Here, ρ is the density, S is salinity, and T is temperature, with reference values $S_0 = 35$ psu and $T_0 = 0$°C.

η_{ref}, the reference height, is determined from Eqn. 1. Note that the reference height can be converted to pressure by multiplying η_{ref} by $\rho_b g$, where ρ_b is deep near-bottom density. Using the methodology outlined above, we calculate η_{ref} at a reference pressure of 2023 dbar (2000 m depth). We emphasize η_{ref} is useful in easily identifying regions of low- and high-pressure, representative of cyclones (blue contours) and anticyclones (red contours), respectively (see Fig. 2a). Although referred to as deep, these eddies are nearly depth-independent in the water column, and are dominant below the pycnocline.

2.3 Complex Empirical Orthogonal Function Analysis

EOF analysis is used to identify prominent spatial and temporal patterns of variability using a principal component analysis, where the data are decomposed into orthogonal eigenvectors (principal components). These eigenvectors illustrate spatial structure for a given mode, and the time-series of each mode are described by the principal coefficients. Modes are ordered according to percent variance, represented by the eigenvalue of the corresponding eigenvector. Much like an EOF, a CEOF describes patterns of variability temporally and spatially; however, they also allow for describing propagation tendencies of prominent features (Horel, 1984).

We conduct a CEOF analysis on deep eddies using the 18 years of daily $\eta_{ref}(x,y,t)$ fields. Deep eddy spatial features are displayed using the modulus of the modes. The phase angle indicates the spatial propagation of the mode, with propagation in the direction of increasing phase angle. Lastly, the mode coefficients indicate the temporally varying strength of the mode. The deep field may be reconstructed as the sum of the products of mode coefficients, times the complex conjugate of mode spatial structures.

3 Deep Eddy Statistics

Figure 2a shows an 18-year mean η_{ref} field with a strong deep cyclone in the DSC and a weaker deep eddy dipole along 26° N near the Mississippi Fan, both features are consistent with previous RAFOS (Pérez-Brunius et al., 2018) and PIES/CPIES observations (Donohue et al., 2016; Johnson Exley et al., 2022). The DSC cyclone is intermittent, with area-mean ($\langle\eta_{ref}\rangle$) ranging from about -0.06 m (cyclonic) to 0.02 m (anticyclonic) and a temporal mean of -0.013 m (Fig. 2c). Figure 2b demonstrates that deep eddy variance in η_{ref} is highest in the eastern Gulf basin just east of the Mississippi Fan (near 26°N,

https://doi.org/10.5194/egusphere-2026-4505
Preprint. Discussion started: 30 July 2026

86°W), again consistent with prior observations (Hamilton et al., 2016; Donohue et al., 2016; Pérez-Brunius et al., 2018; Johnson Exley et al., 2022). Enhanced variance also appears on the Mississippi Fan and in the DSC.

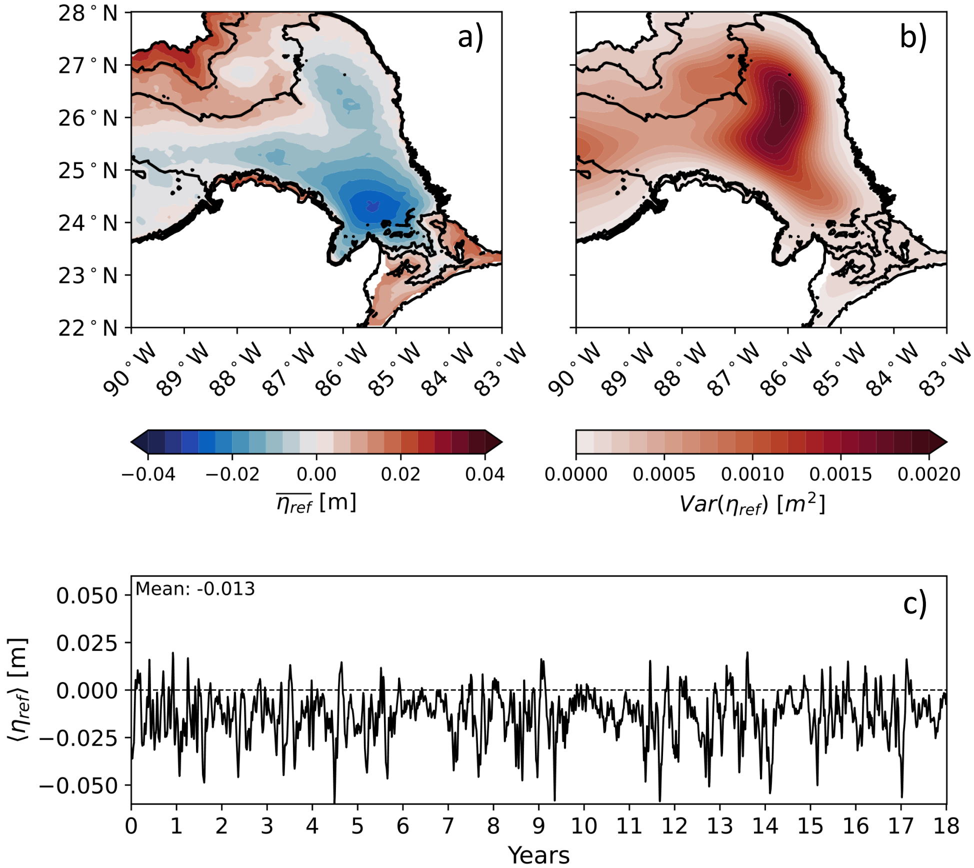

Figure 2. 18-year a) mean and b) variance of η_{ref} in the Eastern Gulf. In a) colored contours correspond to cyclones (negative; blue) and anticyclones (positive; red). Bathymetry is contoured every 500 meters from 2000 to 3500 meters depth. c) 18-year time-series of area-averaged η_{ref} ($\langle\eta_{ref}\rangle$) in the Deep Southeast Channel (DSC), defined as the region bounded by 23.5°N to 25°N and 86.25°W to 84°W. The DSC temporal mean in the region is $\langle\overline{\eta_{ref}}\rangle = -0.013$ m. Negative (positive) values of $\langle\eta_{ref}\rangle$ correspond to cyclonic (anticyclonic) features, the zero line is provided for reference (black, dashed line).

3.1 Spectral Analysis

To better understand deep eddy time scales, we conduct a frequency-spectrum analysis on η_{ref}. Six sites are selected which represent regions of interest based on the 18-year mean and variance of η_{ref} (inset of Fig. 3). Three sites reside in the basin of the Eastern Gulf: the center of the variance hot spot seen in Fig. 2b (green triangle), directly south at the edge of the region of high variance (orange diamond), and just east of the Mississippi Fan (light-blue circle). The remaining three sites include the

https://doi.org/10.5194/egusphere-2026-4505
Preprint. Discussion started: 30 July 2026

DSC (red cross), on the Mississippi Fan (blue square), and in a region of notable variance heading towards the Western Gulf (purple star). Figure 3a displays the frequency-spectrum analysis in a variance preserving plot, from which we identify three frequency bands of interest: $1/150$ - $1/60$ days^{-1}, $1/60$ - $1/30$ days^{-1} and $1/30$ - $1/10$ days^{-1}.

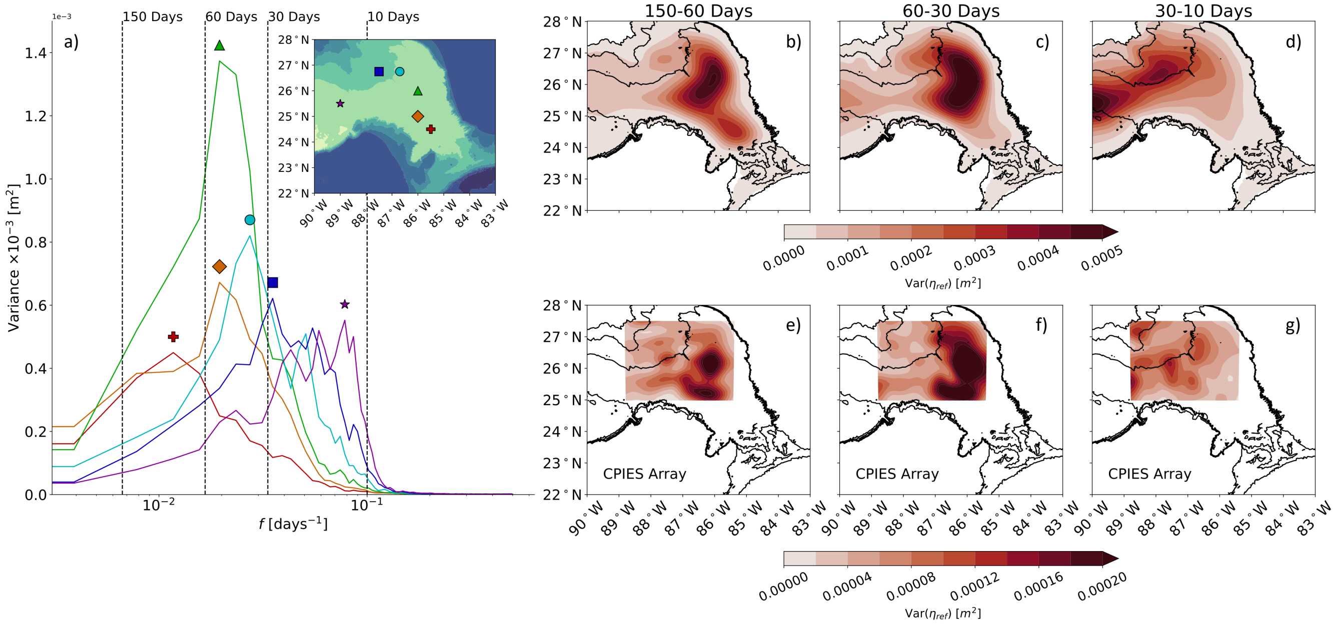

Figure 3. a) Variance preserving frequency spectra at six sites, chosen based on mean and variance of η_{ref} (Fig. 2), including the DSC (red cross), three locations in the basin of the Eastern Gulf (orange diamond, green triangle, and light-blue circle), on the Mississippi Fan (blue square), and towards the Western Gulf (purple star). Inset shows position relative to bathymetry. b-g) Variance of η_{ref} within the three identified frequency bands for the 18-years of model data (top row) and two-years of CPIES observations (Johnson Exley et al., 2022). Note the difference in variance range between the model and observations. Bathymetry are contoured in black every 500 meters from 2000-3500 m depth.

Eddies within the three frequency bands are found in different regions of the Eastern Gulf: $60-150$ day eddies are found east of the Mississippi Fan and in the DSC, $10-30$ day eddies are found on the southern slope of the Mississippi Fan and propagate towards the Western Gulf, and $30-60$ day eddies are concentrated between these regions. The lowest frequency band, $1/150$ - $1/60$ days^{-1}, contains one spectral peak, related to eddies in the DSC (red cross), but both the center of the highest-variance region (green triangle) and the region directly south (orange diamond), also demonstrate significant energy contained within this frequency band (Fig. 3a). Isolating the $60-150$ day variance of η_{ref} (Fig. 3b), we find a similar pattern as seen in Fig. 2b; however, there is elevated variance in the DSC region reinforcing the conclusion that eddies in that region contain lower frequency energy. Moreover, the $60-150$ day variance implies these eddies in the Eastern Gulf basin, which contain low frequency energy, propagate towards the DSC, this will be shown later. Similar patterns of η_{ref} variance in this frequency band are also found in the observations (Fig. 3e). Focusing now on the $1/60$ - $1/30$ days^{-1} frequency band, the

https://doi.org/10.5194/egusphere-2026-4505
Preprint. Discussion started: 30 July 2026

three points in the Eastern basin of the Gulf (orange diamond, green triangle, and light-blue circle) and the Mississippi Fan (blue square) demonstrate significant energy (Fig. 3a). The $30-60$ day variance (Fig. 3c) exhibits a nearly identical pattern as Fig. 2b, with high values in the Eastern Gulf basin, and elevated values near the Mississippi Fan (at 26°N and 87°W). Compared to the low frequency band, there is significantly less variance in the DSC, indicating $30-60$ day eddies propagate from the Mississippi Fan into the basin towards the Campeche Bank. Much like the model, the observations in this frequency band (Fig. 3f) have high variance in the Eastern Gulf basin and near the Mississippi Fan. The Mississippi Fan (blue square) and the region near the Western Gulf (purple star) contain spectral peaks in the highest frequency band, $1/30$ - $1/10$ days^{-1}. In their numerical simulations, Oey (2008) demonstrated high frequency deep eddies were found in a similar location to our purple star site. This is reflected in the variance which is mostly contained on the southern slope of the Mississippi Fan and near the Western Gulf (Fig. 3d); similarly, the observations (Fig. 3g) show elevated variance along the 3000 m isobath and significantly lower variance in the basin, compared to the lower frequency bands. The variance in Fig. 3d,g least resembles the pattern seen in the total variance.

Note, the variance of η_{ref} in the model is higher than in the observations, yet the eddy kinetic energy for the model is lower (see Fig. 6a,d in Morey et al. (2020)); a review of the spatial correlation of η_{ref} at the CPIES locations in the model indicates the model eddies are larger, resulting in weaker pressure gradients and velocities. Why η_{ref} is elevated is unclear. To test whether the observations occurred during a particularly quiet time, we sub-sampled the model over the CPIES domain in two-year segments and compared two-year η_{ref} variance and deep EKE. Probability density function plots showed 12% of two-year segments fell at or near the observed variance in η_{ref}, whereas 80% of two-year model segments fell at or below the observed deep EKE, indicating the observations did not necessarily occur at particularly quiet times. We cannot explain the elevated η_{ref} variance in the model, and this remains a question for future work. Nevertheless, the spatial representation of the variance is consistent between the model and observations, allowing for us to still gain insights into the deep eddy variability.

4 Deep Mesoscale Eddies Pathways

We conduct a CEOF analysis on η_{ref} to identify prominent deep spatial features, and their propagation tendencies. The data are 10-day low-pass filtered to remove small-scale and high-frequency variability. The first three modes which contain 65% of the total variance, constituting 35%, 21%, and 9%, respectively are presented in Fig. 4. These modes are related to the three frequency bands identified from the spectrum analysis, with the first mode mainly containing variance in the $1/60$ - $1/30$ days^{-1} band, and the second and third modes representing variance found in both the low and high frequency bands. Spatial features are displayed using the normalized amplitude (Figs. 4a-c), their propagation tendencies with the phase angle (Figs. 4d-f), and their temporal amplitudes with the CEOF coefficients (Fig. 4g). The propagation is only shown for regions of normalized amplitude ≥ 0.2.

The first mode (Fig. 4a,d) contains 35% of the of the total variance. The spatial amplitude of this mode looks similar to the total variance (Fig. 2b) – as well as the variance in the $1/60$ - $1/30$ days^{-1} band (Fig. 3c). Eddies represented by this mode appear to originate at the edge of the Mississippi Fan (near 27°N and 86.5°W) and propagate towards the Eastern Gulf

https://doi.org/10.5194/egusphere-2026-4505
Preprint. Discussion started: 30 July 2026

basin. Donohue et al. (2016) highlighted this region as a place where strong deep eddy kinetic energy could be generated through baroclinic development, and Le Hénaff et al. (2012) suggested numerically an upper cyclone could generate a deep eddy through interactions with the topography of the Mississippi Fan. We conjecture the first mode represents eddies formed through similar mechanisms, containing energy in the $1/60$ - $1/30$ days^{-1} band. There is no indication they propagate towards the DSC, instead moving towards the basin of the Eastern Gulf, then west.

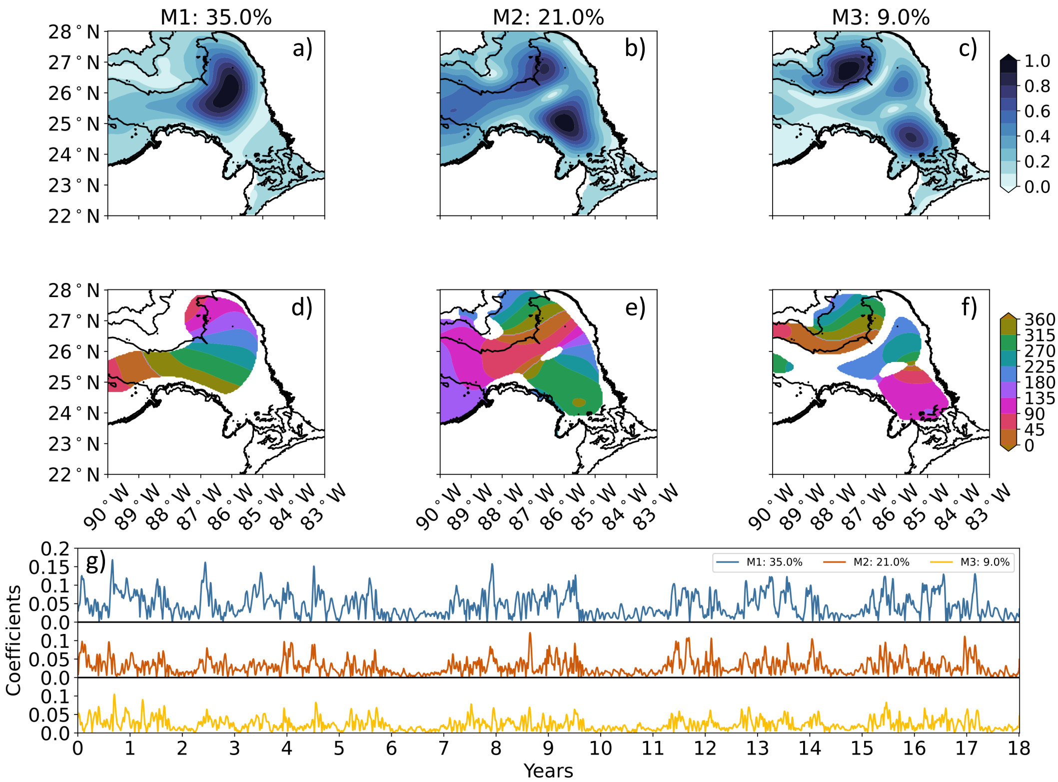

Figure 4. CEOF analysis of 10-day low-pass filtered η_{ref}. a-c) Normalized amplitudes, d-f) phase angles, and g) CEOF coefficients of the first three modes. High amplitude regions (dark blue-black) in a-c) indicate prominent spatial features; regions where normalized amplitude is < 0.2 are masked in d-f). Features propagate with increasing phase in d-f), *i.e.*, from pink to purple to blue to green. First, second, and third mode temporal coefficients in g) are represented by blue, orange, and yellow, respectively.

The second mode (Figs. 4b,e) describes 21% of the variance, and is largest in two regions: the DSC and the Mississippi Fan (about $27°$N and $86.5°$W). The DSC variability is related to the deep cyclone (Figs. 2a,c). Phase here shows a large area of a single phase (green region) consistent with a standing feature, with some slight tendency to propagate north and west along the bathymetry of the Campeche Bank. The elevated region along the southeast base of the Mississippi Fan propagates south southeast, parallel to the West Florida Shelf. These eddies represented by the second mode are most likely to contain

https://doi.org/10.5194/egusphere-2026-4505
Preprint. Discussion started: 30 July 2026

$60-150$ day energy, reflected by the peak in the frequency spectrum in the $1/150$ - $1/60$ days^{-1} band (Fig. 3a), as well as the heightened $60-150$ day variance in the DSC (Fig. 3b).

Much like the second mode, the third mode (Figs. 4c,f) – representing 9% of the total variance – also describes elevated variance in the DSC and on the Mississippi Fan; including a feature between the two. The feature on the Mississippi Fan has the strongest amplitude, and based on the phase (Fig. 4f) is prevalent between the 2500-3000 m isobath, propagating westward. The eddies represented by this spatial feature are associated with high frequency energy in the $1/30$ - $1/10$ days^{-1} band, due to the presence of the spectral peak from the Mississippi Fan (blue square; Fig. 3a) and the variance found in this band (Fig. 3c). This finding is strongly supported by Johnson Exley et al. (2022), who found a similar large amplitude feature and propagation pattern in this region in their CEOF analysis of η_{ref} in a $1/20$ - $1/10$ days^{-1} frequency band. Like the second mode, the phase associated with the DSC circulation contains a single phase (magenta region), representing a standing feature; however, unlike the second mode the DSC feature does not appear connected to the cyclones that originate near the Mississippi Fan and propagate south towards the DSC.

The three modes found with the CEOF analysis explain 65% of the total variance of the deep eddies in the Eastern Gulf, represented by η_{ref}. The first mode, appears to be associated with eddies containing energy in the $1/60$ - $1/30$ days^{-1} band which form through baroclinic development near the Mississippi Fan, and propagate towards the deep eastern basin, then west. The second mode is likely related to low frequency energy eddies in the $1/150$ - $1/60$ days^{-1} band generated by baroclinic development near the Mississippi Fan that propagate south towards the DSC, whereas the third mode represents eddies with high frequency energy in the $1/30$ - $1/10$ days^{-1} band – constrained by the 2500 and 3000 m isobath – and a standing feature containing low frequency energy in the DSC.

4.1 Implications for the Loop Current System

Deep, mesoscale eddies in the Gulf interact with the LC system through an upper-lower layer coupling (Donohue et al., 2016; Hamilton et al., 2016, 2019). We now review how their variability influences LCE separation events. The LC length (kilometers) and its northernmost extension (°N) over the 18-years of the simulation are presented in Fig. 5. Both metrics are useful in identifying times when the LC has detached or separated, as well as identifying where the LC is in relation to topographic features of interest. We differentiate between full LCE separations and detachment events using pink, solid lines to mark separation times. Over the 18-years reviewed, we identify sixteen separation events, defined as times the LC experienced a sudden decrease in length (≥ 200 km), and sustained this drop in length for ≥ 28 days. Lindo-Atichati et al. (2013) also used a 28 day cut-off to identify LCE separations when analyzing satellite altimetry observations and found good agreement with previous works. This somewhat strict definition ignores smaller separations – where the LC releases small tip LCEs – yet remains significantly extended into the Gulf, and detachment-reattachment events which are not included in our analysis.

The temporal coefficients of the CEOF analysis (Fig. 4g) indicate when each mode is intensified, so we define a threshold of one standard deviation above the mean for each of the three time-series to identify periods when each mode is most intense (peaking), and is thus highly representative of the deep η_{ref} field at that time. These peak time periods are added as color-filled blocks above the LC length and LC northern extension time-series (Fig. 5) with Mode 1 (blue) in the top row, Mode 2 (orange)

https://doi.org/10.5194/egusphere-2026-4505
Preprint. Discussion started: 30 July 2026

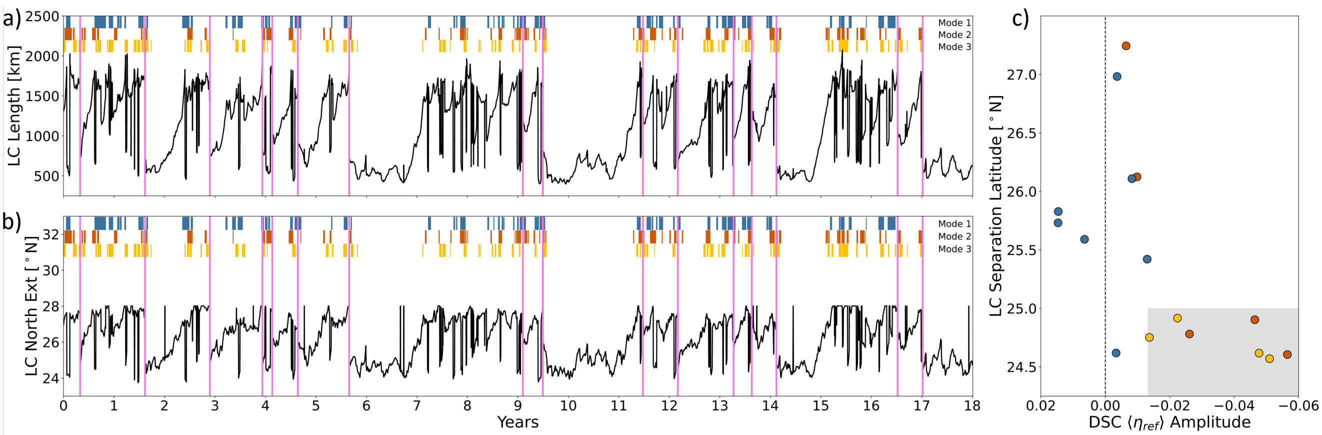

Figure 5. Time-series (black, solid lines) of a) LC length and b) northernmost extension of the LC. Pink, solid lines indicate separation times. Blue, orange, and yellow blocks marked along the top are associated with Modes 1, 2, and 3, respectively, at times where the modes are most intense. c) Latitude of LC at separation versus area-averaged strength of η_{ref} in the DSC at separation. Symbols are colored to indicate the mode which persists most over a 30-day separation window. Black, dashed line separates mean cyclonic ($\langle\eta_{ref}\rangle < 0$) from anticyclonic ($\langle\eta_{ref}\rangle > 0$) circulation in the DSC.

in the middle, and Mode 3 (yellow) on the bottom row; this provides a visual to better diagnose how the η_{ref} field looks during detachments and separations. The most apparent result is the lack of mode peaks during times when the LC is retracted. Note the absence of the mode peaks in Years 6, 10, 14, and 17, which saw extended periods in which the LC remained below 27°N – approximately the extent needed to encounter the topography of the Mississippi Fan (see Fig. 5b). In contrast, when the LC is extended and appears to detach or separate, mode peaks are more apparent (Fig. 5a). The LC northern extent and length, along with the intensification of the modes, indicate the topographic interactions with the Mississippi Fan play a key role for the development of deep, mesoscale eddies, and contribute to almost all LCE separations.

During a detachment or separation, we find the three modes can exist both jointly and independently. To get a better sense for the role of the modes during a separation event, we define a dominant mode. This is determined as the mode peak which persists longest in a 30-day window centered about the separation day; in no case do two modes persist for the same amount of time in this window. Further, a 30-day window centered about a separation, as opposed to 30-days prior to a separation, is justified in that the modes – and the energy in their corresponding eddies – do not immediately dissipate once a LCE is separated; they may persist. Recognizing that the magnitude of the coefficients (Fig. 4g) decreases with each mode, we also normalized each time-series by their standard deviation (not shown) and reanalyze when the modes intensify and are dominant, finding no difference with the preceding analysis.

We plot the latitude of the LC at separation versus $\langle\eta_{ref}\rangle$ in Fig. 5c. Symbols for each separation are colored by the dominant mode during that separation, as described above. We highlight below three key observations developed out of this figure:

https://doi.org/10.5194/egusphere-2026-4505
Preprint. Discussion started: 30 July 2026

i. LCE separations in the presence of a strong ($\langle\eta_{ref}\rangle \leq -0.013$ m) deep cyclone in the DSC region occur south of 25°N (gray shaded region).

ii. Separations when a strong deep cyclone exists in the DSC are dominated by the second or third mode.

iii. Separations with weaker or no cyclonic features in the DSC, tend to be dominated by the first mode and typically maintain separations north of 25°N.

Monitoring the DSC cyclone could provide a predictive measure for separation latitude. Figure 5c shows a predictive threshold could be developed that indicates high probability of a southern separation.

5 Conclusions

We review the variability of deep, mesoscale eddies in the Eastern Gulf of Mexico using 18-years from a 54-year regional HYCOM free running simulation. Using the reference pressure component of the sea surface height, η_{ref}, to identify eddies, we analyzed the mean and variance of the deep eddy variability in the Eastern Gulf (Fig. 2), with the mean displaying a deep cyclone in the Deep Southeast Channel (DSC). The variance of η_{ref} indicated high variability in the basin of the Eastern Gulf, and a frequency-spectrum analysis (Fig. 3a) in regions of enhanced variance revealed three frequency bands of $1/150$ - $1/60$ days^{-1}, $1/60$ - $1/30$ days^{-1}, and $1/30$ - $1/10$ days^{-1}. Variance of deep eddies containing energy within these bands (Fig. 3b-d) exhibited different regional preferences: $60-150$ day eddies showed high variance in the Eastern Gulf basin and the DSC, $10-30$ day eddies presented highest variance on the Mississippi Fan, while $30-60$ day eddies displayed enhanced variance near the Mississippi Fan and the Eastern Gulf basin with little variance in the DSC. Observations displayed similar patterns of deep variance in these frequency bands (Fig. 3e-g). Complex empirical orthogonal function (CEOF) analysis (Fig. 4) on η_{ref} identified three modes containing 65% of the total variance, with the modes describing propagation patterns of deep eddies in the differing frequency bands. The first mode resembled the total variance (Fig. 2b) and described eddies which develop near the Mississippi Fan, likely due to baroclinic development, and propagated into the Eastern Gulf basin and then west. These eddies likely contain energy in the $1/60$ - $1/30$ days^{-1} band. The second and third modes identified the DSC as a region of elevated variance, with the former indicating a propagation pathway of eddies – in the $60-150$ day band – from the Mississippi Fan to the DSC and the latter displaying a $60-150$ day standing feature in the DSC. The third mode also displayed heightened variance on the southern slope of the Mississippi Fan, indicative of $10-30$ day eddies (Fig. 3d), which develop on the Mississippi Fan and propagate westward.

Using the CEOF temporal coefficients, we identified times when the three modes intensified and related these time-periods to time-series of the Loop Current (LC) length and its northern extension (Fig. 5a,b). Notably, we find an absence of these intense mode time-periods when the LC is in a retracted state, not interacting with the topography of the Mississippi Fan, suggesting the LC is integral to the development and intensification of the deep cyclones; instead, the modes tend to peak during times where the LC is detaching or separating. To better understand this relationship between the modes and LC separations, we reviewed the latitude of the LC at separation versus the area-averaged η_{ref} in the DSC, $\langle\eta_{ref}\rangle$, and identified the mode which

https://doi.org/10.5194/egusphere-2026-4505
Preprint. Discussion started: 30 July 2026

persists longest during the separation (Fig. 5c). Separations having strong deep cyclones in the DSC, with $\langle \eta_{ref} \rangle \leq -0.013$ m, are associated with the second and third modes and separate south of 25°N. When the DSC lacks a strong cyclone, separations are associated with the first mode and occur north of 25°N.

This work highlights a need for sustained deep observations in the Eastern Gulf, especially in the under-sampled Deep Southeast Channel region. Deep cyclones in the DSC influence LC Eddy (LCE) separation events (Safaie et al., 2025), with particular influence on separation latitude. Our results demonstrate the importance of an extended Loop Current that interacts with the topography of the Mississippi Fan and energizes deep circulation (see Fig. 5a,b). The CEOF analysis provides evidence of pathways for cyclones forming off the Mississippi Fan to propagate south towards this region. More work is needed to understand these processes. Moreover, Cooke et al. (2025) found lower uncertainty in the deep field initial condition of regional Gulf of Mexico ensemble forecasts led to improved forecasts. Deep observations should also be included in model and forecast data assimilation, to constrain the deep fields.

Code and data availability. Jupyter Notebooks for data access and conducting the analysis are available at doi.org/10.5281/zenodo.21608468. Model data used in this study can be found at hycom.org. Bottom pressure data collected from the CPIES array can be found at data.griidc.org.

Author contributions. J.P.C., K.A.D., and D.R.W. designed the study. K.A.D. and D.R.W. acquired funding for the study. J.P.C., K.A.D., and D.R.W. determined the methods to be used in the study. J.P.C. wrote the code and conducted the data analysis. J.P.C. wrote the first draft of the manuscript. J.P.C., K.A.D., and D.R.W. contributed to editing and revising the manuscript.

Competing interests. The authors declare that they have no conflict of interest.

Acknowledgements. J.P.C., K.A.D., and D.R.W. acknowledge funding from the US National Academy of Science, Engineering, and Medicine (NASEM) under their Gulf Research Program, UGOS grants, 2000009943 and 200013145.

https://doi.org/10.5194/egusphere-2026-4505
Preprint. Discussion started: 30 July 2026

References

Abascal, A., Sheinbaum, J., Candela, J., Ochoa, J., and Badan, A.: Analysis of flow variability in the Yucatan Channel, Journal of Geophysical Research: Oceans, 108, 2003.

Bunge, L., Ochoa, J., Badan, A., Candela, J., and Sheinbaum, J.: Deep flows in the Yucatan Channel and their relation to changes in the Loop Current extension, Journal of Geophysical Research: Oceans, 107, 26–1, 2002.

Cooke, J., Donohue, K., Rowley, C. D., Thoppil, P. G., and Watts, D. R.: The Role of Deep Mesoscale Eddies in Ensemble Forecast Performance, arXiv preprint arXiv:2511.09747, 2025.

Donohue, K., Watts, D., Hamilton, P., Leben, R., and Kennelly, M.: Loop Current Eddy formation and baroclinic instability, Dynamics of Atmospheres and Oceans, 76, 195–216, 2016.

Dukhovskoy, D. S., Leben, R. R., Chassignet, E. P., Hall, C. A., Morey, S. L., and Nedbor-Gross, R.: Characterization of the uncertainty of Loop Current metrics using a multidecadal numerical simulation and altimeter observations, Deep Sea Research Part I: Oceanographic Research Papers, 100, 140–158, 2015.

Hamilton, P.: Topographic Rossby waves in the Gulf of Mexico, Progress in Oceanography, 82, 1–31, 2009.

Hamilton, P., Lugo-Fernández, A., and Sheinbaum, J.: A Loop Current experiment: Field and remote measurements, Dynamics of Atmospheres and Oceans, 76, 156–173, 2016.

Hamilton, P., Bower, A., Furey, H., Leben, R., and Pérez-Brunius, P.: The Loop Current: Observations of deep eddies and topographic waves, Journal of Physical Oceanography, 49, 1463–1483, 2019.

Horel, J.: Complex principal component analysis: Theory and examples, Journal of Applied Meteorology and Climatology, 23, 1660–1673, 1984.

Johnson Exley, A., Donohue, K. A., Watts, D. R., Tracey, K. L., and Kennelly, M. A.: Generation of high-frequency topographic Rossby waves in the Gulf of Mexico, Frontiers in Marine Science, 9, 1049 645, 2022.

Larrañaga, M., Jouanno, J., Chassignet, E. P., Durante, G., Ma, I., Sheinbaum, J., and Renault, L.: The role of cyclonic eddies in the detachment and separation of Loop Current eddies, Ocean Science, 22, 821–841, 2026.

Le Hénaff, M., Kourafalou, V. H., Morel, Y., and Srinivasan, A.: Simulating the dynamics and intensification of cyclonic Loop Current Frontal Eddies in the Gulf of Mexico, Journal of Geophysical Research: Oceans, 117, 2012.

Leben, R. R.: Altimeter-derived Loop Current metrics, Geophysical Monograph-American Geophysical Union, 161, 181, 2005.

Lindo-Atichati, D., Bringas, F., and Goni, G.: Loop Current excursions and ring detachments during 1993–2009, International Journal of Remote Sensing, 34, 5042–5053, 2013.

Manta, G., Durante, G., Candela, J., Send, U., Sheinbaum, J., Lankhorst, M., and Laxenaire, R.: Predicting the Loop Current dynamics combining altimetry and deep flow measurements through the Yucatan Channel, Frontiers in Marine Science, 10, 1156 159, 2023.

McKinney, L. D., Shepherd, J. G., Wilson, C. A., Hogarth, W. T., Chanton, J., Murawski, S. A., Sandifer, P. A., Sutton, T., Yoskowitz, D., Wowk, K., et al.: The gulf of mexico, Oceanography, 34, 30–43, 2021.

Morey, S. L., Gopalakrishnan, G., Sanz, E. P., Azevedo Correia De Souza, J. M., Donohue, K., Pérez-Brunius, P., Dukhovskoy, D., Chassignet, E., Cornuelle, B., Bower, A., et al.: Assessment of numerical simulations of deep circulation and variability in the Gulf of Mexico using recent observations, Journal of Physical Oceanography, 50, 1045–1064, 2020.

National Academies of Sciences and Medicine: Understanding and predicting the Gulf of Mexico Loop Current: critical gaps and recommendations, National Academies Press, 2018.

https://doi.org/10.5194/egusphere-2026-4505
Preprint. Discussion started: 30 July 2026

Oey, L.-Y.: Loop Current and deep eddies, Journal of physical oceanography, 38, 1426–1449, 2008.

Olvera-Prado, E. R., Moreles, E., Zavala-Hidalgo, J., and Romero-Centeno, R.: Upper–lower layer coupling of recurrent circulation patterns in the Gulf of Mexico, Journal of Physical Oceanography, 53, 533–550, 2023.

Pérez-Brunius, P., Furey, H., Bower, A., Hamilton, P., Candela, J., García-Carrillo, P., and Leben, R.: Dominant circulation patterns of the deep Gulf of Mexico, Journal of Physical Oceanography, 48, 511–529, 2018.

Rosburg, K. C., Donohue, K. A., and Chassignet, E. P.: Three-dimensional model-observation comparison in the Loop Current region, Dynamics of Atmospheres and Oceans, 76, 283–305, 2016.

Safaie, A., Donohue, K., Rowley, C. D., Thoppil, P. G., and Watts, D. R.: Deep Cyclones in the Southeast Gulf of Mexico, Frontiers in Marine Science, 12, 1648 949, 2025.

Sheinbaum, J., Athié, G., Candela, J., Ochoa, J., and Romero-Arteaga, A.: Structure and variability of the Yucatan and loop currents along the slope and shelf break of the Yucatan channel and Campeche bank, Dynamics of Atmospheres and Oceans, 76, 217–239, 2016.

Sturges, W. and Leben, R.: Frequency of ring separations from the Loop Current in the Gulf of Mexico: A revised estimate, Journal of Physical Oceanography, 30, 1814–1819, 2000.

Taira, K., Brunton, S. L., Dawson, S. T., Rowley, C. W., Colonius, T., McKeon, B. J., Schmidt, O. T., Gordeyev, S., Theofilis, V., and Ukeiley, L. S.: Modal analysis of fluid flows: An overview, AIAA journal, 55, 4013–4041, 2017.

Thoppil, P. G., Rowley, C. D., Hogan, P. J., and Stear, J.: Evaluating the performance of an ensemble forecast system in predicting Loop Current Eddy separation in the Gulf of Mexico, Progress in Oceanography, p. 103529, 2025.

Tsei, S., Howden, S., Diercks, A.-R., Zhang, J. A., Miles, T. N., Nyadjro, E., and Martin, K. M.: Low salinity, high ocean heat content, and warm core eddy effects on the upper ocean response during Hurricane Sally (2020): An analysis of a Hurricane Glider observations and coupled atmosphere-ocean model, Journal of Geophysical Research: Oceans, 130, e2024JC021 470, 2025.